

**SEMI-ANNUAL REPORT**

(for July - December 1995)

Contract Number NAS5-31363



**OCEAN OBSERVATIONS WITH EOS/MODIS:**

**Algorithm Development and Post Launch Studies**

Howard R. Gordon  
University of Miami  
Department of Physics  
Coral Gables, FL 33124

(Submitted January 16, 1996)

**Abstract**

Several significant accomplishments were made during the present reporting period.

- An investigation of the influence of stratospheric aerosol on the performance of the atmospheric correction algorithm is nearly complete. The results indicate how the performance of the algorithm is degraded if the stratospheric aerosol is ignored. Use of the MODIS 1380 nm band to effect a correction for stratospheric aerosols was also studied. Simple algorithms such as subtracting the reflectance at 1380 nm from the visible and near infrared bands can significantly reduce the error; however, only if the diffuse transmittance of the aerosol layer is taken into account.
- The atmospheric correction code has been modified for use with absorbing aerosols. Tests of the code showed that, in contrast to nonabsorbing aerosols, the retrievals were strongly influenced by the vertical structure of the aerosol, even when the candidate aerosol set was restricted to a set appropriate to the absorbing aerosol. This will further complicate the problem of atmospheric correction in an atmosphere with strongly absorbing aerosols.
- Our whitecap radiometer system and solar aureole camera were both tested at sea and performed well.
- Investigation of a technique to remove the effects of residual instrument polarization sensitivity were initiated and applied to an instrument possessing ~ 3-4 times the polarization sensitivity expected for MODIS. Preliminary results suggest that for such an instrument, elimination of the polarization effect is possible at the required level of accuracy by estimating the polarization of the top-of-atmosphere radiance to be that expected for a pure Rayleigh scattering atmosphere. This may be of significance for design of a follow-on MODIS instrument.
- W.M. Balch participated on two month-long cruises to the Arabian sea, measuring coccolithophore abundance, production, and optical properties. A thorough understanding of the relationship between calcite abundance and light scatter, in situ, will provide the basis for a generic suspended calcite algorithm.

**1. Atmospheric Correction Algorithm Development.**

**a. Task Objectives:**

During CY 1995 there are five objectives under this task:

(i) Investigate the effects of stratospheric aerosol and/or cirrus clouds on the performance of the proposed atmospheric correction algorithm.

(ii) Complete a multilayer Monte Carlo simulation code that includes the effects of aerosol and molecular scattering polarization (a vector radiative transfer code) and sea surface roughness.

(iii) Investigate the effects of ignoring the polarization of the atmospheric light field on the performance of the proposed atmospheric correction algorithm.

(iv) Investigate the effects of vertical structure in the aerosol concentration and type on the behavior of the proposed atmospheric correction algorithm.

(v) Begin a detailed investigation of the performance of the correction algorithm in atmospheres with strongly absorbing aerosols.

**b. Work Accomplished:**

(i) Considerable progress was made regarding the influence of stratospheric aerosols on atmospheric correction, and the possibility of using the 1380 nm MODIS band for removing their effects. A new report covering the present status of this work is attached as Appendix 1. This supersedes that attached to the last Semi-Annual Report. Basically, it was found that including the one-way diffuse transmittance of the stratospheric aerosol made a considerable improvement in using the 1380 nm band for removal of stratospheric effects.

(ii) We have completed development and validation of a multilayer Monte Carlo code radiative transfer code that includes polarization and reported on its performance in the last Semi-Annual Report.

(iii) Using the Monte Carlo simulation code in (ii) above, we started a study of the error in the atmospheric correction algorithm caused by ignoring polarization. The results were described in the last Semi-Annual Report. As the effects of ignoring polarization appeared to be small compared to other problems, we postponed this aspect of our work in favor of concentrating on vertical structure and absorbing aerosols using the much-faster two-layer and three-layer scalar radiative transfer codes.

(iv) As described in (iii), we decided to utilize our simpler and faster two-layer and three-layer scalar radiative transfer codes to begin an examination of the effects of vertical structure. The goal was to explore the range of the effect to determine which aspect on which to focus the work to be carried out with the more complete but much slower code. This proved very fitful.

Briefly, the reflectance of the atmosphere in the single-scattering approximation is independent of the manner in which the aerosol is distributed with altitude. However, this independence does

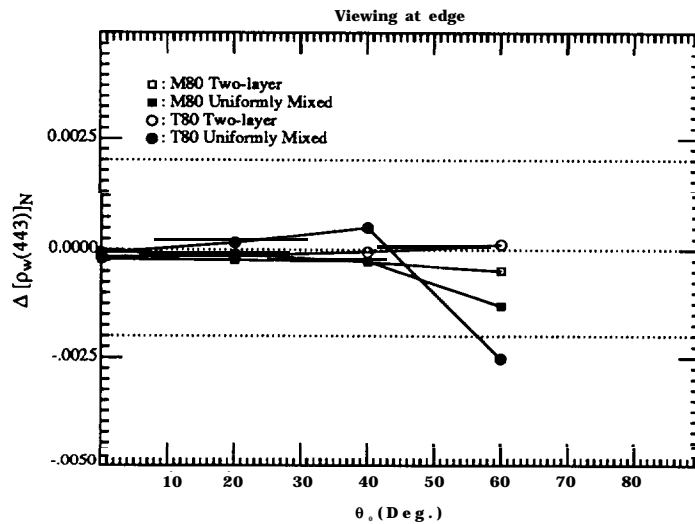


Figure 1. Effect of the vertical distribution of aerosol on  $\Delta [p_w(443)]_N$  as a function of the solar zenith angle,  $\theta_s$ , at the edge of the scan for the T80 and M80 aerosol models with  $\tau(865) = 0.2$ . Note that the correction algorithm assumes that the "Two-layer" stratification is correct.

not extend to a multiple-scattering atmosphere. As the multiple-scattering atmospheric correction algorithm assumes that the aerosol is all located in the bottom layer of a two-layer atmosphere, it

is important to understand the effect of aerosol vertical structure on the correction algorithm. This has been studied by comparing the error in the algorithm when pseudo data are simulated using the “correct” two-layer model with the error when the pseudo data are simulated using a model in which the aerosol and molecular number densities have an altitude-independent mixing ratio, i.e., a uniformly mixed model. Figure 1 provides such a comparison for the M80 and T80 aerosol models with  $\tau_a(865) = 0.2$ . ( “M80”, “T80”, and the “U” models used below refer to the *Shettle and Fenn* [1979] Maritime and Tropospheric models at 80% relative humidity, and their Urban models at the indicated relative humidity, respectively. )  $\Delta [p(443)]_N$  is the error in the water-leaving reflectance at 443 nm. The goal of atmospheric correction is that the magnitude of  $\Delta [p(443)]_N$  be less than 0.002. As these two vertical structures represent the extreme limits that might be found in nature, we conclude that the effect of an incorrect assumption regarding the vertical structure will not lead to serious errors in this case. However, as we shall see in (v), when the aerosol is strongly absorbing, the effects of vertical structure are very large.

(v) We have started a systematic study of the effects of absorbing aerosols on the performance of the atmospheric correction algorithm. Recall that that the algorithm as presently configured uses a set of 12 candidate aerosol models based on the work of *Shettle and Fenn* [1979]. These models range from nonabsorbing to weakly-absorbing aerosols. However, the presence of strongly absorbing aerosols, such as urban pollution carried by the winds over the Middle Atlantic Bight in summer, or Saharan dust transported over the Tropical North Atlantic, the algorithm does not perform well. Figure 2a compares the performance of the algorithm when the pseudo data is generated by the M80, C80, T80, and U80 aerosol models. In the figure,  $E^{(e)}(765, 865)$  is the estimated value of the aerosol reflectance ratio between 765 and 865 nm. It is fundamental to the operation of the atmospheric correction algorithm [Gordon and Wang, 1994]; however, it is unnecessary for the purposes of this discussion, and the reader should focus on  $\Delta [p(443)]_N$ . The first three models are

similar, but not identical to, members of the candidate aerosol set. For these, the correction is

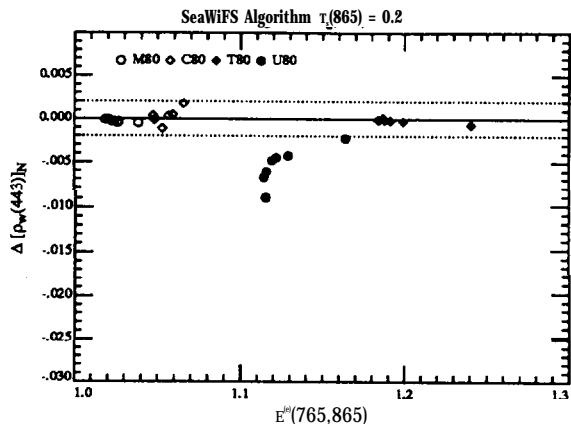


Figure 2a.  $\Delta [p_w(443)]_N$  as a function of  $E^s(765,865)$  for  $\tau_s(865) = 0.2$  and all of the viewing geometries examined in the study, using the multiple-scattering algorithm.

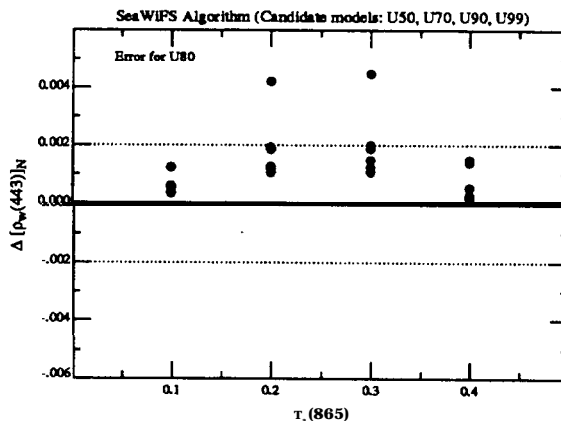


Figure 2b.  $\Delta [p_w(443)]_N$  as a function of  $\tau_s(865)$  for the U80 model, when the candidate aerosol models in the multiple-scattering algorithm are restricted to U50, U70, U90, and U99.

excellent. In contrast, the correction of the U80 model is very poor. The poor performance is due to the fact that the presence of strong absorption significantly alters the magnitude of the multiple scattering effects from that expected for the nonabsorbing or weakly-absorbing aerosols. Thus, strongly absorbing aerosols must be included in the candidate aerosol set. To test the efficacy of this, we made a set of multiple scattering lookup tables based on four candidate models U50, U70, U90, and U99. The results of the correction algorithm using these candidates are presented in Figure 2b. Note that the maximum error in Figure 2b is only twice the minimum error in Figure 2a. Unfortunately, if the strongly- and weakly-absorbing candidate aerosol models are mixed, the algorithm fails because it is impossible to directly determine whether or not the aerosols in an image are strongly absorbing. Thus, it appears that it is necessary to develop sets of candidate models based on a climatology of aerosol properties.

Using this restricted set of candidate models, we have also investigated the effect of vertical

structure of the aerosol. These results are presented in Figure 3. Figure 3a provides the two-layer

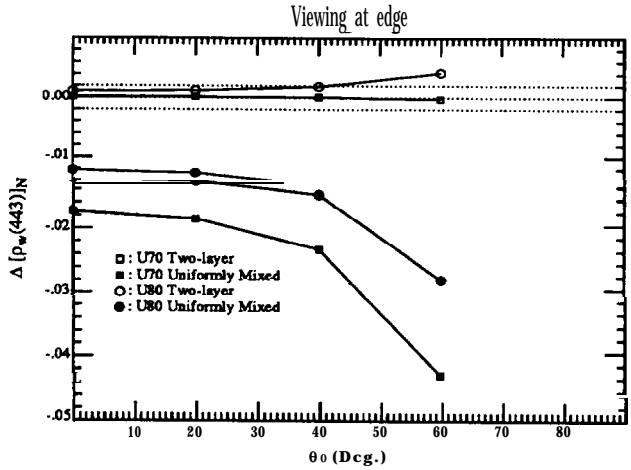


Figure 3a. Effect of the vertical distribution of aerosol on  $\Delta [p_w(443)]_N$  as a function of  $\theta_0$  at the edge of the scan for the U80 and U70 aerosol models with  $\tau_a(865) = 0.2$ . The "Uniformly Mixed" case refers to a constant mixing ratio between the aerosol and molecular number densities. The "Two-layer" case places the aerosol at the sea surface as assumed by the correction algorithm.

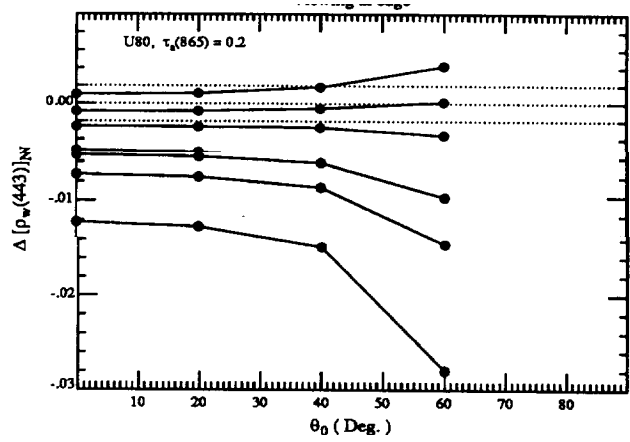


Figure 3b. Effect of the vertical distribution of aerosol on  $\Delta [p_w(443)]_N$  as a function of  $\theta_0$  at the edge of the scan for the U80 aerosol models with  $\tau_a(865) = 0.2$ . Curves from top to bottom refer to situations in which the aerosol is confined to a layer just above the surface, between the surface and 1, 2, 4, and 6 km, and uniformly mixed throughout the atmosphere.

versus uniformly mixed cases for the Urban models with  $\tau_a(865) = 0.2$ . In this case the candidate aerosol models were restricted to U50, U70, U90, and U99, as in the results for Figure 2b. For the U80 case, the error becomes excessive, increasing by over an order of magnitude compared to the two-layer case. More disturbing is the performance of the U70 aerosol model. U70 is actually one of the candidate aerosol models in this case. When the vertical structure is the same as assumed by the algorithm, the error is negligible. In contrast, when the incorrect structure is assumed, the error becomes very large,

As we have examined only an extreme deviation from that assumed by the correction algorithm, it is of interest to quantify how the correction algorithm performs as the aerosol layer thickens from being confined just near the surface to being mixed higher in the atmosphere. Thus, the top-of-atmosphere reflectance was simulated using a two layer model with aerosol *plus* Rayleigh scattering in the lower layer and *only* Rayleigh scattering in the upper layer. The fraction of the Rayleigh scattering optical thickness assigned to the lower layer was consistent with aerosol-layer thickness of 0, 1 km, 2 km, 4 km, 6 km, and infinity. The aerosol model used in the simulations was U80, and

$\tau_a(865)$  was kept constant at 0.2. The multiple-scattering algorithm was then operated with this pseudo data using U50, U70, U90, and U99 as candidate models. The results of this exercise are provided in Figure 3b. Clearly, progressive thickening of the layer in which the aerosol resides leads to a progressive increase in the error in the retrieved water-leaving reflectance. The figure suggests that it would be necessary to know the layer thickness to within  $\pm 1$  km, *as well as* to use the proper candidate model set in order to provide a correction with the desired accuracy.

This influence of vertical structure on the algorithm when the aerosol is strongly absorbing is easy to understand. The algorithm assumes all of the aerosol resides in a thin layer beneath the molecular scattering layer. As the aerosol layer thickens and encompasses more and more of the molecular scattering layer, the amount of Rayleigh scattering within the aerosol layer will increase causing an increase in the average path length of photons through the layer, and a concomitant increase in absorption. Thus, for a given  $\tau_a$ , the top-of-atmosphere reflectance,  $p_r$ , will decrease as the thickness of the aerosol layer increases. Since the Rayleigh scattering component of the reflectance,  $p_r \sim \lambda^{-4}$ , this decrease will be relatively more in the visible than in the NIR., and the algorithm will incorrectly assess the aerosol contribution.

Finally, we have begun examining the MODIS SWIR bands as a means for detecting the presence of strongly absorbing aerosols, mainly dust transported by the winds to the marine environment from desert areas, e.g., Saharan dust. At present there is no way to effect this; however, computations using Mie scattering suggest that MODIS observations of  $p_t(\lambda)$  for  $\lambda > 865$  nm, may be useful in this regard. Figure 4 compares the  $\epsilon(\lambda, 865)$  for Haze C distributions (standard Junge power-law distributions, with number density  $8 \text{ diameter}^{-3}$ ) of nonabsorbing (liquid water) and absorbing (minerals transported over the oceans with the index of refraction taken from *d'Almeida, Koepke and Shettle* [1991]) aerosol particles. Also included on Figure 4 are computations for a log-normal distribution suggested in *d'Almeida, Koepke and Shettle* [1991] for minerals transported over large distances to the marine environment. In the figure,  $\epsilon(\lambda, 865)$  is the ratio of the single-scattered aerosol reflectance at a wavelength  $\lambda$  to that at 865 nm. It is a key parameter in the atmospheric correction algorithm. In contrast to nonabsorbing aerosols, the mineral aerosol shows a significant decrease in  $\epsilon(\lambda, 865)$  for  $\lambda > 1.26 \text{ } \mu\text{m}$  over that extrapolated from the observed

$\epsilon(765, 865)$  and  $\epsilon(1260, 865)$ . This behavior of  $\epsilon(\lambda, 865)$  is apparently due to the rapid decrease in the real part of the mineral refractive index beyond 1260 nm. Notwithstanding the perils of using Mie theory to predict the large-angle scattering for irregularly shaped particles [Mishchenko and

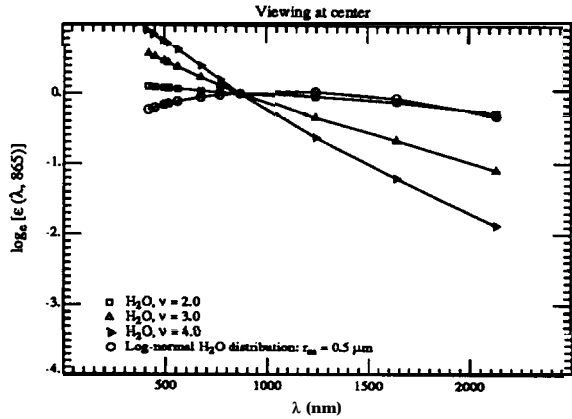


Figure 4a.  $\epsilon(\lambda, 865)$  for nadir viewing with  $\theta_0 = 60^\circ$  for the Haze C models composed of liquid water.

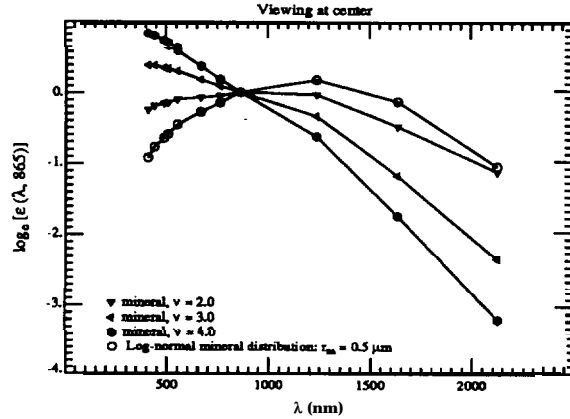


Figure 4b.  $\epsilon(\lambda, 865)$  for nadir viewing with  $\theta_0 = 60^\circ$  for the Haze C models composed of absorbing minerals.

Travis, 1994; Mugnai and Wiscombe, 1989] these computations suggest that it may be reasonable to try to use the short-wave infrared (SWIR) bands on MODIS to differentiate between some types of absorbing and nonabsorbing aerosols.

c. Data/Analysis /Interpretation: See item b above.

d. Anticipated Future Actions:

(i) We expect to finish this work in the next quarter and submit a paper to *Applied Optics*.

(ii) None. This task is now complete.

(iii) We will continue work on the effect of polarization on atmospheric correction.

(iv) We will continue work on the vertical structure problem, particularly for absorbing aerosols. Using more realistic vertical structures, we will try to estimate the accuracy with which the vertical structure is required to effect an acceptable atmospheric correction.

**MODIS Semi-Annual Report (1 July – 31 December 1995) Contract NAS5-31363**

(v) We will continue investigating the possibility of utilizing the MODIS SWIR bands to differentiate between weakly- and strongly-absorbing aerosols. Not only is this important for the purpose of improving atmospheric correction, but also important for possibly providing a means for identifying imagery for which the quality of the atmospheric correction may be degraded, i.e., for quality assurance. However, much of the work on absorbing aerosols will be directed toward the vertical structure problem discussed under (iv).

**Additional tasks for CY96.** The basic correction algorithm yields the product of the diffuse transmittance  $t$  and the water-leaving reflectance  $p_w$ . However,  $t$  depends on the angular distribution of  $p_w$ . If  $p_w$  were uniform,  $t$  would be easy to compute, and this approximation has always been employed in the past. In a series of papers Morel and Gentili [Morel and Gentili, 1991; Morel and Gentili, 1993] studied theoretically the bidirectional effects as a function of the sun-viewing geometry and the pigment concentration. Their simulations suggest that, although the bidirectional effects nearly cancel in the estimation of the pigment concentration using radiance ratios,  $p_w$  can depend significantly on the solar and viewing angles. (Our major task number 3, a study of the in-water radiance distribution, experimentally addresses this problem. ) We have initiated a study to understand the effect of bidirectional effects on the diffuse transmittance. This will be an area of intense work during CY 96.

**e. Problems/Corrective Actions:**

(i) None.

(ii) None.

(iii) None.

(iv) None.

(v) None.

**f. Publications:**

**MODIS Semi-Annual Report (1 July - 31 December 1995) Contract NAS5-31363**

H.R. Gordon, Atmospheric Correction of Ocean Color Imagery in the Earth Observing System Era, Submitted to *Journal of Geophysical Research, Atmospheres*.

**2. Whitecap Correction Algorithm (with K.J. Voss),**

**a. Task Objectives:**

As described in earlier reports, a whitecap radiometer system has been built and tested to provide a database for the development and validation of the whitecap correction algorithm. The database includes spectral information as well as variables associated with the formation and occurrence of whitecaps such as wind speed, air/sea temperature, and global position.

**b. Work Accomplished:**

Construction, integration and calibration of the whitecap radiometer, deck cell and meteorology package has been completed. The complete system was initially tested on two one-day cruises locally in Florida waters. Although whitecaps were scarce the system simultaneously acquired the full suite of data as expected: 6 channels downwelling irradiance and upwelling radiance, air/water temperature, wind speed and direction, GPS data and UTC time. In addition, a color TV video camera mounted beside the radiometer head relayed and recorded the water, waves and whitecaps passing below. The video image was time and date stamped whenever the radiometer and the rest of the system acquired data. This provided a frame by frame reference for subsequent analysis.

In the second half of October the system was deployed on the RV McGaw for a 14-day cruise off the coast of Southern California. Weather conditions were primarily calm with diffuse overcast days — not the best for whitecap formation. However, data was taken of foam generated by the ship's wake as it moved from test station to test station. The radiometer was mounted in different positions over the side of the ship providing a data base for radiometer performance and analysis of different stages of foam development.

In early November the whitecap system was deployed on the RV Moana Wave for a 5-day cruise off the coast of the Hawaiian island of Lanai. Higher wind speeds were encountered early in

the morning and late in the evening, with some sporadic and short lived periods during the day. All in all, not many whitecaps were observed by the system to generate a good statistical database to correlate fractional coverage with wind speed or air/water temperature. This was probably due to our close proximity to the island during the cruise which most likely caused the variable and short-lived winds as well as sheltering effects.

c. Data/Analysis/Interpretation:

As stated above, spectral reflectance of foam obtained by observation of the ship's wake as it moved from test station to test station was acquired and an example of the data is shown in Figure 5. Augmented reflectance in Figure 5 is defined as the total measured reflectance minus the water

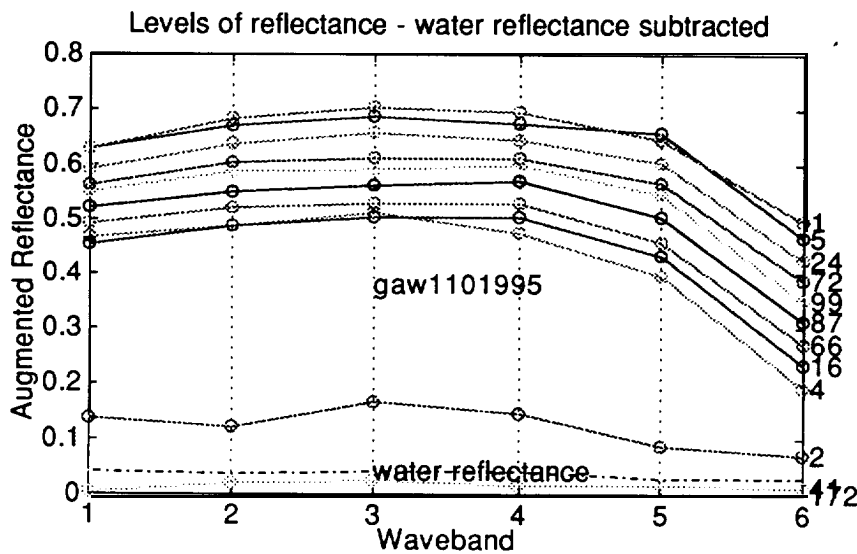


Figure 5. Spectral reflectance of a ship wake.

and sky reflectance, i.e., the reflectance of the foam and submerged bubbles. The magnitude of the augmented reflectance varies due to variations in the passing foam from submerged bubbles to thick surface foam layers. In this example, the radiometer primarily observed thick surface foam layers. The numbers on the right of the graph indicate the number of data points averaged within a certain interval of waveband 6 reflect ante values. Wavebands 1 through 6 correspond to wavelengths 410,

440, 510, 550, 670 and 860 nm respectively. The water reflectance (including sky reflectance) that has been subtracted is indicated by the dash-dot line.

Interesting features to note are: (i) the consistency of the spectral shape for differing reflectance values, (ii) the drop off in bands 1 and 2, (iii) some foam reflect ante values approaching 70% in bands 3 and 4. The drop off in bands in 5 and 6 are understood to be due the absorption of water at those wavelengths and should drop off more quickly when observing submerged bubbles and foam [Schwindling, 1995]. The drop off in bands 1 and 2 could be due to the absorption of yellow substance and has yet to be confirmed. The mean reflectance value of foam from this data set approaches 60% in bands 3 and 4, and is in agreement with those values found in the literature [Stabeno and Monahan, 1986]. However, reflectance values as high as 70% have been measured.

In the next example (Figure 6) data from a naturally occurring whitecap, are provided. The

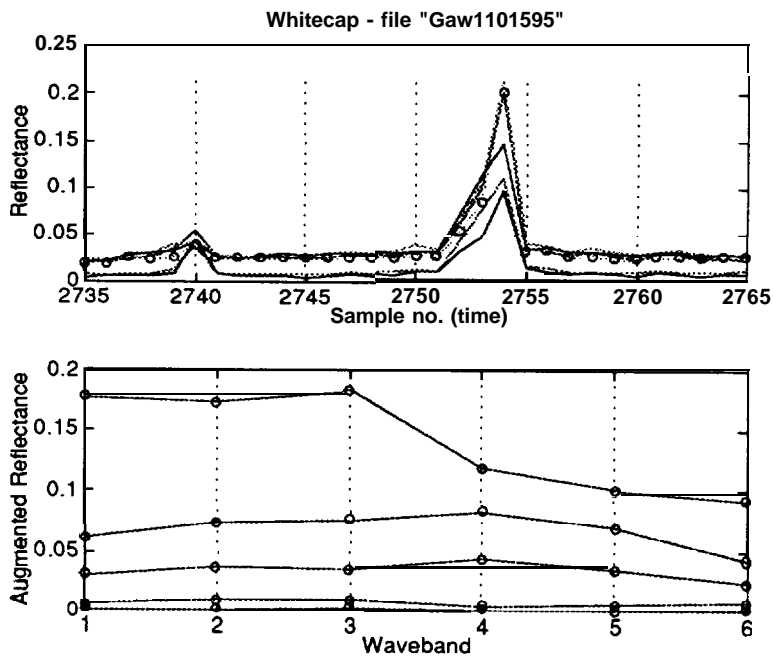


Figure 6. Spectral reflectance of a whitecap.

upper panel in Figure 6 is a continuous record of reflect ante versus sample number (time). A whitecap occurs at sample points 2752 to 2754. The augmented reflect ante values for the individual

**MODIS Semi-Annual Report (1 July - 31 December 1995) Contract NAS5-31363**

wavebands are in the lower panel for sample points 2751 through 2755. The maximum reflectance value for the whitecap occurred between sample points 2753 and 2754, and was not acquired by the radiometer. The spectral shape of sample points 2752 and 2753 is consistent with the spectral shape of foam found from ship wake data. Sample point 2754 drops sharply at waveband 4. This sample point observes mainly residual (streaky) foam from the disintegrating whitecap and is most likely due to observation by that spectral channel of a slightly different area than that of the other channels.

**d. Anticipated Future Actions:**

In order to enhance the database to correlate fractional whitecap coverage with wind speed and air/ water temperature, the video image (having a greater field of view than the radiometer) can be digitized so that the quantity of white foam pixels in every  $n^{\text{th}}$  video frame can be calculated. Calculating the ratio of white foam pixels to total pixels in every  $n^{\text{th}}$  video frame, over a sufficient number of video frame images acquired under the same wind speed, air/water temperature should provide a sufficient database to relate the whitecap coverage to wind speed, etc. This requires the procurement of a video frame grabber and software designed to analyze existing and future data, and we will be investigating this in the next period. Additional sea data will also be acquired, and we will be arranging cruises in appropriate e locations.

**e. Problems/Corrective Actions:** None.

**3. In-water Radiance Distribution (with K.J. Voss).**

**a. Task Objectives:**

The main objective in this task is to obtain upwelling radiance distribution data at sea for a variety of solar zenith angles to understand how the water-leaving radiance varies with viewing angle and sun angle.

**b. Work accomplished:**

## **MODIS Semi-Annual Report (1 July – 31 December 1995) Contract NAS5-31363**

We used the R.ADS [Voss, 1989] instrument during the previously mentioned October cruise in Hawaii. The system had been augmented with polarizers to acquire the in-water polarized radiance distribution. During this cruise the system had a grounding problem and did not work, however we brought the instrument out for a short check out during another cruise in December and the instrument worked properly.

**c. Data/Analysis/Interpretation:** none

**d. Anticipated future actions:**

We will be looking for another opportunity to acquire data at sea as soon as possible. This will probably be another cruise with Dennis Clark in the Spring, or another short cruise off of Miami during this period.

**e. Problems/Corrective actions:** None.

**f. Publications:**

A. Morel, K.J. Voss, B. Gentili, Bidirectional reflectance of oceanic waters: A comparison of modeled and measured upward radiance fields, *Journal of Geophysical Research*, 100C, 13,143–13,150 (1995).

### **4. Residual Instrument Polarization.**

**a. Task Objectives:**

The basic question here is: if the MODIS responds to the state of polarization state of the incident radiance, given the polarization-sensitivity characteristics of the sensor, how much will this degrade the performance of the algorithm for atmospheric correction? Now that we have the capability of computing the polarization state of the top-of-atmosphere radiance, we shall begin to study this question. We will examine the visible sensors on MSX, which will probably be the first in-space instrument that can provide MODIS-like data. This instrument has greater polarization sensitivity than is anticipated for MODIS, so it should provide an excellent test of our methodology.

**b. Work Accomplished:**

We have developed a formalism [Gordon, 1988] which provides the framework for removal of instrumental polarization-sensitivity effects. The difficulty with removing the polarization sensitivity error is that the polarization properties of the radiance backscattered by the aerosol are unknown. Although the details of the correction process have yet to be determined, simulations of this effect for an instrument possessing ~ 3-4 times the polarization sensitivity expected for MODIS are presently being carried out. Preliminary results suggest that elimination of the polarization effect is possible at the required level of accuracy by estimating the polarization of the top-of-atmosphere radiance to be that expected for a pure Rayleigh scattering atmosphere.

**c. Data/Analysis/Interpretation:**

See **b** above.

**d. Anticipated Future Actions:**

We will apply our techniques to MODIS.

**e. Problems/Corrective Actions: None**

**f. Publications: None.**

**5. Direct Sun Glint Correction.**

**a. Task Objectives: None.**

**6. Prelaunch Atmospheric correction validation (with K.J. Voss).**

**a. Task Objectives:**

The long-term objectives of this task are two-fold. First, we need to study the aerosol phase function and its spectral variation in order to verify the applicability of the aerosol models used in the atmospheric correction algorithm. Effecting this requires obtaining long term time series

**MODIS Semi-Annual Report (1 July - 31 December 1995) Contract NAS5-31363**

of the aerosol optical properties in typical maritime environments. This will be achieved using a CIMEL sun/sky radiometer that can be operated in a remote environment and send data back to the laboratory via a satellite link. These are similar the radiometers used by B. Holben and Y. Kaufman. Second, we must be able to measure the aerosol optical properties from a ship during the initialization/calibration/validation cruises. The CIMEL-type instrumentation cannot be used (due to the motion of the ship) for this purpose. The required instrumentation consists of an all-sky camera (which can measure the entire sky radiance, with the exception of the solar aureole region, from a moving ship), an aureole camera (specifically designed for ship use) and a hand-held sun photometer. We have a suitable sky camera and sun photometer and had to construct an aureole camera. Our objective for this calendar year was (1) to assemble, characterize, and calibrate the solar aureole camera system, (2) to develop data acquisition software, and (3) to test the system. A second objective was to acquire a CIMEL Automatic Sun Tracking Photometer, calibrate it, and deploy it in a suitable location for studying the optical properties of aerosols over the ocean.

**b. Work Accomplished:**

We have constructed the solar aureole camera system, tested the system in the lab, and during October tested the instrument on a short cruise off Hawaii. The instrument worked fairly well in the Hawaii test, where several sample data sets with both the aureole camera and sky radiance distribution camera system were obtained. While preliminary data reduction has shown that the instrument performed well, there were two areas which needed improvement. Specifically, both the data acquisition triggering of the individual frames, and the filter changing, need to be improved.

The CIMEL instrument was sent to B. Holbren (NASA/GSFC) to be calibrated in comparison with his other instruments before being sent in the field. Several problems were found with the instrument, so this process took much longer than expected. At present we still hope to have a CIMEL installed in the Dry Tortugas before the end of the quarter, but if not it will be installed soon after the beginning of the new quarter.

**c. Data/Analysis/Interpretation: None.**

**d. Anticipated Future Actions:**

We will have a CIMEL instrument installed in its location in the Dry Tortugas very soon. We will also reduce the Aureole data and sky radiance data obtained during the October cruise during the next quarter.

We have initiated a critical examination of the effect of radiative transfer on "vicarious" calibration exercises. In particular, we are trying to determine the accuracy with which the radiance at the top of the atmosphere can be estimated based on measurements of sky radiance and aerosol optical thickness at the sea surface. We are carrying out a complete sensitivity analysis of the transfer process including the effects of earth curvature, polarization, sea surface roughness, and calibration error in the surface-based radiometer.

**e. Problems/corrective actions: None.**

**f. Publications:**

H.R. Gordon and T. Zhang, Columnar Aerosol Properties Over Oceans by Combining Surface and Aircraft Measurements: Simulations, *Applied Optics*, 34,5552-5555 (1995).

H. Yang, H.R. Gordon and T. Zhang, Island perturbation to the sky radiance over the ocean: Simulations *Applied Optics* (in press)

**7. Detached Coccolith Algorithm and Post Launch Studies (W.M. Baich).**

**a. Task Objectives:**

The algorithm for retrieval of the detached coccolith concentration from the coccolithophorid, *E. huxleyi* is described in detail in our ATBD. The key is quantification of the backscattering coefficient of the detached coccoliths. Our earlier studies focussed on laboratory cultures to understand factors affecting the calcite-specific backscattering coefficient. To this end, the objectives of

our coccolith studies have been, under conditions of controlled growth of coccolithophores (using chemostats), to define the effect of growth rate on:

- (1) the rate that coccoliths detach from cells (this is also a function of turbulence and physical shear),
- (2) rates of coccolith production
- (3) morphology of coccoliths
- (4) volume scattering and backscatter of coccoliths

During early 1995, our work focussed on making many of the measurements to address these four objectives. Many of the data will be analyzed in 1996.

In the latter half of 1995, our work focused on shipboard measurements of suspended calcite and estimates of optical backscatter as validation of the laboratory measurements. We participated on two month-long cruises to the Arabian sea, measuring coccolithophore abundance, production, and optical properties. A thorough understanding of the relationship between calcite abundance and light scatter, in situ, will provide the basis for a generic suspended calcite algorithm. As with algorithms for chlorophyll, and primary productivity, the natural variance between growth related parameters and optical properties needs to be understood before the accuracy of the algorithm can be determined.

**b. Work Accomplished:**

During this last 6 months, we have performed mostly shipboard studies in the Arabian Sea. Beginning in April, we have been preparing for these cruises, shipping most of the laboratory to Muscat, Oman. In mid-July, we departed Bigelow Laboratory for Muscat, then sailed aboard the R/V Thomas Thompson for 30 days during the SW Monsoon. We sampled standing stocks, and calcification rates of coccolithophores. Samples were taken for microscopic enumeration of plated coccolithophores as well as detached coccoliths. Standing stocks of suspended calcite were also sampled on precombusted filters for later analysis using graphite furnace atomic absorption. These

**MODIS Semi-Annual Report (1 July - 31 December 1995) Contract NAS5-31363**

samples still must be run. Finally, calcification rates were measured using a new micro-diffusion  $C^{14}$  technique. Such measurements provide perhaps the best estimate of how rapidly coccoliths are produced in the sea. This cruise returned to Muscat at the end of August.

On 20 October, we returned to Muscat for the second cruise (intermonsoon) which lasted until the end of November. We performed all of the measurements made during the first cruise, plus the weather conditions allowed us to use our new underway light scatter detection system. This device sampled the non-toxic seawater line of the ship for temperature, salinity, pH, chlorophyll fluorescence, and volume scattering (before and after the addition of a weak acid to dissolve the calcite). All data are averaged and logged every kilometer of the 3500 km trip.

The cruise also involved towing an Undulating Oceanographic Recorder (UOR) which provided the vertical resolution to our surface underway studies. The UOR is towed with about 500 m of cable, and undulates over the top 100 m, providing a complete CTD profile with associated optics (up-looking and down-looking irradiance detectors at the SEAWiFS wavelengths) every 1.5 km of the 3500 km trip.

**c. Data/Analysis /Interpretation:**

Given the considerable time at sea, no major data analysis has been performed yet.

**d. Anticipated Future Actions: Most of the data** analysis will take place in the next year. The current state of the data is as follows:

- (1) Suspended calcite samples still need to be run in the graphite furnace. We are currently learning operation of the instrument.
- (2) Some 600 cell and coccolith counts need to be performed.
- (3) All calcification data have been processed to units of  $gC\ m^{-3}\ d^{-1}$  and integrated over the water column at each station. They still need to be processed into complete sections.

- (4) Turnover of the calcite particles needs to be calculated.
- (5) The underway data is now processed for temperature, salinity, pH, fluorescence and backscatter (with and without calcite) averaged over each kilometer of the trip. The data currently are in files representing each leg of the 26 leg trip. Following final calibration checks, the data will be assembled into one file.
- (6) Of major interest in this data set will be the relationship between calcite-dependent backscatter ( $b'_p$ ) and the concentration of suspended calcite or concentration of detached coccoliths. This will be of major relevance to our MODIS algorithm efforts. Besides actually checking our algorithm, the net result will be an idea of the accuracy and precision of the algorithm, exceedingly important for subsequent interpretation.

**e. Problems/Corrective Actions: None**

**f. Publications:**

Our first paper to Limnology and Oceanography on coccolithophore bio-optics has been revised and returned to the journal. The second paper of the series is being revised now.

**8. Other Developments.**

A study of the effect of a bright target (such as a cloud), in the field of view of the MODIS, on the behavior of the atmospheric correction and bio-optical algorithms was carried out. Near-field scatter data provided by MCST was combined with simulations of the top-of-atmosphere clear-sky radiance over the ocean to effect the study for the protoflight instrument. The results were forwarded to Wayne Esaias for transmittal to the Team Leader.

**9. Publications and submissions for CY 95.**

**MODIS Semi-Annual Report (1 July - 31 December 1995) Contract NAS5-31363**

The following publications in CY 95 received support from the present contract.

K. Ding and H.R. Gordon, Analysis of the influence of O<sub>2</sub> "A" band absorption on atmospheric correction of ocean color imagery, *Applied Optics*, 34, 2068-2080 (1995).

H.R. Gordon and T. Zhang Columnar Aerosol Properties Over Oceans by Combining Surface and Aircraft Measurements: Simulations. *Applied Optics*, 34, 5552-5555 (1995).

M. Wan and H.R. Gordon, Estimation of aerosol columnar size distribution and optical thickness from the angular distribution of radiance exiting the atmosphere: simulations, *Applied Optics*, 34 6989-7001 (1995).

H. Yang, H.R. Gordon and T. Zhang, Island perturbation to the sky radiance over the ocean: Simulations, *Applied Optics* (In Press).

H.R. Gordon, Remote sensing of ocean color: a methodology for dealing with broad spectral bands and significant out-of-band response, *Applied Optics* (In Press).

H.R. Gordon, Atmospheric Correction of Ocean Color Imagery in the Earth Observing System Era, *Journal of Geophysical Research, Atmospheres* (Submitted).

W.M. Balch and K.A. Kilpatrick, The 1991 Coccolithophore Bloom in the Central North Atlantic I. Optical Properties and Factors Meeting Their Distribution, *Limnology and Oceanography*, (Submitted).

W.M. Balch, K.A. Kilpatrick, P. Holligan and D. Harbour, The 1991 Coccolithophore Bloom in the Central North Atlantic II. Relating Optics to Coccolith Concentration, Their Distribution, *Limnology and Oceanography*, (Submitted).

**10. References.**

d'Almeida, G. A., P. Koepke and E. P. Shettle, *Atmospheric Aerosols — Global Climatology and Radiative Characteristics*, A. Deepak Publishing, Hampton, VA, 1991.

Gordon, H. R., Ocean Color Remote Sensing Systems: Radiometric Requirements, *Society of Photo-Optical Instrumentation Engineers, Recent Advances in Sensors, Radiometry, and Data Processing for Remote Sensing*, 924, 151-167, 1988.

Gordon, H. R. and M. Wang, Influence of Oceanic Whitecaps on Atmospheric Correction of SeaWiFS, *Applied Optics*, 33, 7754-7763, 1994.

**MODIS Semi-Annual Report (1 July - 31 December 1995) Contract NAS5-31363**

- Mishchenko, M. I. and L. D. Travis, Light scattering by polydispersions of randomly oriented spheroids with sizes comparable to wavelengths of observation, *Applied Optics*, 33, 7206-7225, 1994.
- Morel, A. and B. Gentili, Diffuse reflectance of oceanic waters: its dependence on Sun angle as influenced by the molecular scattering contribution, *Applied Optics*, 30, 4427-4438, 1991.
- Morel, A. and B. Gentili, Diffuse reflectance of oceanic waters. II. Bidirectional aspects, *Applied Optics*, 32, 6864-6879, 1993.
- Mugnai, A. and W. J. Wiscombe, Scattering from nonspherical Chebyshev particles. 3: Variability in angular scattering patterns, *Applied Optics*, 28, 3061-3073, 1989.
- Schwindling, M., Modeles et mesures pour l'observation spatiale de la couleur de l'ocean: Diffusion atmospherique par les aerosols et reflexion de surface par l'ecume, 1995, Docteur de L'Universite these, Univ. des Sci. et Tech. de Lille. 245 pp.
- Shettle, E. P. and R. W. Fenn, Models for the Aerosols of the Lower Atmosphere and the Effects of Humidity Variations on Their Optical Properties, Air Force Geophysics Laboratory, Hanscomb AFB, MA 01731, AFGL-TR-79-0214, 1979.
- Stabeno, P. J. and E. C. Monahan, The Influence of Whitecaps on the albedo of the Sea Surface, in *Oceanic Whitecaps*, edited by E. C. Monahan and G. M. Niocaill, pp. 261-266, Reidel, Dordrecht, 1986.
- Voss, K. J., Electro-optic Camera System for Measurement of the Underwater Radiance Distribution, *Optical Engineering*, 28, 241-247, 1989.